

Rheology and structures of aqueous gels of diblock(oxyethylene–oxybutylene) copolymers with lengthy oxyethylene blocks

Antonios Kellarakis,^a Withawat Mingvanish,^b Christophe Daniel,^c Hong Li,^b Vasiliki Havredaki,^a Colin Booth,^{*b} Ian W. Hamley^c and Anthony J. Ryan^d

^a National and Kapodistrian University of Athens, Department of Chemistry, Physical Chemistry Laboratory, Panepistimiopolis, 157 71 Athens, Greece

^b Department of Chemistry, University of Manchester, Manchester, UK M13 9PL

^c School of Chemistry, University of Leeds, Leeds, UK LS2 9JT

^d Department of Chemistry, University of Sheffield, Sheffield, UK S3 7HF

Received 25th February 2000, Accepted 14th April 2000

Published on the Web 18th May 2000

Aqueous solutions of diblock copolymers $E_{96}B_{18}$, $E_{184}B_{18}$, $E_{315}B_{17}$ and $E_{398}B_{19}$ (E = oxyethylene unit, B = oxybutylene unit) were investigated by rheometry and small-angle X-ray scattering (SAXS). Storage (G') and loss (G'') modulus and yield strength (σ_y) were used to define hard- and soft-gel phases in experiments which covered the concentration range 2–14 wt.% copolymer. Values of G' correlated with those of yield strength, the ratio G'/σ_y being *ca.* 0.03. SAXS was used to explore hard-gel structures, and to confirm hard-gel/soft-gel boundaries. The sol/soft-gel boundary was identified as a percolation threshold. The effect of an increase in E-block length was to move the gel phases to lower concentrations without changing the pattern of their behaviour. In this respect, the critical conditions for hard-gel formation (c^* , T^*) served as parameters for a 'universal' phase diagram.

1 Introduction

Block copolymers of poly(oxyethylene) and a hydrophobic poly(oxyalkylene) in dilute aqueous solutions can form micelles, and in more concentrated solutions can form liquid-crystal mesophases (gels). The most familiar copolymers of this type are the $E_mP_nE_m$ triblocks, where we use E to denote an oxyethylene unit, OCH_2CH_2 , and P an oxypropylene unit, $OCH_2CH(CH_3)$, while n and m denote number-average block lengths in repeat units. These copolymers are available from a number of commercial sources, including BASF Corp., Uniqema (formerly ICI surfactants), Serva AG and Hoechst AG. The phase behaviours, structures and rheological properties of these gels have been well researched in recent years, and this work has been reviewed.^{1–3} Notable contributions are initial studies by Schmolka and Bacon,⁴ broad surveys of phase behaviour by Wanka *et al.*,^{5,6} structural studies by Mortensen and co-workers,^{7–10} rheological studies by Hvidt and co-workers^{11,12} and a theoretical study by Noolandi *et al.*¹³

Aqueous gels of block copolymers of ethylene oxide and 1,2-butylene oxide have also been investigated. The work has included a comparative study of copolymers with linear diblock and triblock architectures: E_mB_n , $E_mB_nE_m$ and $B_nE_mE_mB_n$.¹⁴ [B denotes the oxybutylene chain unit, $OCH_2CH(C_2H_5)$.] A limited range of E_mB_n and $E_mB_nE_m$ copolymers is available from The Dow Chemical Co.,¹⁵ but many more have been synthesised in Manchester. Studies of diblock E_mB_n copolymer aqueous gels have been reported from our laboratories (see ref. 16 and citations therein) and elsewhere.¹⁷ Previous work has included aspects of the micellisation and gelation of the copolymers of present interest ($E_{96}B_{18}$, $E_{184}B_{18}$, $E_{315}B_{17}$ and $E_{398}B_{19}$).^{18,19}

In this paper we focus on the rheological properties of

aqueous micellar sols and gels. Of relevant work on $E_mP_nE_m$ copolymers,^{2,6,11,12,20} our work is most closely related to that of Hvidt *et al.*¹¹ on solutions of $E_{21}P_{47}E_{21}$ (coded P94). In describing these complex fluids, they have used yield stress (σ_y), storage (G') modulus and loss (G'') modulus to distinguish three convenient (if arbitrary) subdivisions within the range of behaviours: hard-gel, soft-gel and sol.^{1,11} Observation of a solution on inversion of the tube containing it is a simple method, based on yield stress, for distinguishing mobile from immobile systems. The shear stress on the sample in the inverted tube depends upon the choice of conditions for the test. As practised in our laboratories (see Section 2 for details) a solution with yield stress exceeding 40 Pa will not flow in the test, and can be classified as a hard gel. The method has been shown to give results in excellent agreement with those from rheology and differential scanning calorimetry (DSC),²¹ and we have used it in preliminary surveys of a number of systems.^{22–24} Of the solutions which are mobile in the inverted-tube test, those with zero yield stress and $G'' > G'$ can be classified as true sols. Between these extremes may be found solutions with small but finite yield stress and $G' > G''$, properties which are characteristic of a gel. The values of G' and G'' depend upon choice of frequency, but we have found that experiments at 1 Hz give consistent results.²¹ In keeping with other reports of the rheology of aqueous micellar solutions of block copolymers^{1,11,21} we call this particular Bingham fluid a soft gel.

Considering E_mB_n copolymers, studies of aqueous gel structures have been focused largely on the cubic spherical-micelle phase. These results are reviewed in a recent paper,¹⁹ and the conditions (copolymer concentration, mole ratio of block lengths, m/n) under which the cubic mesophase at room temperature adopts either body-centred cubic (bcc) or face-centred cubic (fcc) symmetry have been defined. For example,

at room temperature 10 wt.% aqueous gels of copolymers $E_{96}B_{18}$ and $E_{184}B_{18}$ have fcc symmetry, while those of copolymers $E_{315}B_{17}$ and $E_{398}B_{19}$ have bcc symmetry.¹⁹

Of the various aqueous gels of E_mB_n copolymers which have been studied, only those of copolymer $E_{41}B_8$ have been investigated by rheometry across a wide range of the phase diagram.²¹ For other E_mB_n copolymers, large-amplitude-oscillatory shear and/or steady shear has been used either to align hard-gel mesophases and so lead to orientation of Bragg reflections in SAXS and SANS studies, or as an end in itself in detailed investigations of shear-induced orientation (and orientational transitions) in structured mesophases (see refs. 16 and 19). Considering the results from rheology and SAXS for copolymer $E_{41}B_8$ in water,^{21,25} the extent of the soft-gel region, and particularly its extension to low temperatures, distinguishes its phase diagram from those published for aqueous solutions of copolymers $E_{21}P_{47}E_{21}$ (P94) and $E_{27}P_{39}E_{27}$ (P85) by Hvidt and co-workers,^{11,12} both of which show a high-temperature soft-gel region coincident with the presence of rod-like micelles: see Section 4.2 for further discussion.

The purpose of the work described in this paper was to examine the generality of the $E_{41}B_8$ type of phase diagram by extending rheological measurements to diblock copolymers with lengthy E-blocks (E_{100} to E_{400}), focusing particularly on the soft-gel regions in the phase diagram. To this end the present experiments covered the concentration range 2–15 wt.% copolymer and the temperature range 5–95 °C. To maintain efficient micellisation at low copolymer concentration, the copolymers were targeted to have B-block lengths of 18. In the event, as noted above, we achieved E_{96} – E_{398} and B_{17} – B_{19} . As already reported¹⁸ (and as seen again in Section 3.1.1) the effect of a long E-block is to move the critical concentration for hard-gel formation to low copolymer concentrations. This effect is related to the increased expansion (swelling) of the poly(oxyethylene) chains in the fringe (corona) of the micelles, and has been quantified in terms of a thermodynamic expansion factor related to the ratio of the excluded volume of a micelle (as measured in dilute solution by light scattering or SANS) to its anhydrous volume.^{16,18,24} The effect of increasing the B-block length is to stabilise micelles against dissociation at low temperatures, and thereby to stabilise the hard-gel phase at low temperatures. [In this respect it is noted that poly(oxyethylene) has a negative temperature coefficient of solubility in water, and so is more soluble in the better solvent at low temperature.] This important effect of hydrophobe-block length, which is discussed in detail elsewhere,²⁶ is of minor importance in the present work on gels of copolymers with similar B-block lengths: *i.e.* B_{17} to B_{19} .

2 Experimental

2.1 Copolymers and gels

The preparation of the copolymers used in this work ($E_{96}B_{18}$, $E_{184}B_{18}$, $B_{315}B_{17}$ and $E_{398}B_{19}$) was by sequential anionic polymerisation of ethylene oxide followed by 1,2-butylene oxide, as described previously.¹⁸ Gel permeation chromatography (GPC) was used to confirm narrow chain length dis-

tributions, and ¹³C NMR spectroscopy was used to obtain absolute values of number-average molar mass, and to confirm the diblock architecture.¹⁸ The molecular characteristics of the copolymers are summarised in Table 1.

To prepare a gel sample, copolymer and water were weighed into a closed vessel, then cooled and allowed to stand for a day or so at *ca.* 10 °C before being transferred rapidly to the appropriate holder, as described below. Occasionally, to aid solubilisation by melting the crystalline copolymer, the mixture was heated to 70 °C before cooling to 10 °C.

2.2 Rheometry

The rheological properties of the samples were determined using a Bohlin CS50 Rheometer with water-bath temperature control. Couette geometry (bob, 24.5 mm diameter, 27 mm height; cup, 26.5 mm diameter, 29 mm height) was used for all the samples, with 2.5 cm³ sample being added to the cup in the mobile state. A solvent trap maintained a water-saturated atmosphere around the cell, and evaporation was not significant for the temperatures and timescales investigated. For example, there was no significant change in response at a given temperature during the heating–cooling programme 65 → 85 → 65 °C covering a period of 3 to 4 h.

Storage and loss moduli were recorded across the temperature range with the instrument in oscillatory-shear mode, usually at a frequency (f) of 1 Hz, but for certain systems across the range 0.1 to 10 Hz. In this mode, the samples were heated at 1 °C min⁻¹ in the range 5–95 °C. For all measurements the strain amplitude was low (<0.5%, linear viscoelastic region), thus ensuring that G' and G'' were independent of strain.

Measurements of yield stress and viscosity were made at selected temperatures with the instrument in steady-shear mode. The instrument was programmed to increase the shear stress in a series of logarithmically-spaced steps, allowing a maximum of 1 min to equilibrate at each step. Usually a period of 20 min was allowed for temperature equilibration before starting the program at any given temperature.

In the related tube-inversion experiments, described previously,¹⁸ samples (0.5 g) were enclosed in small tubes (internal diameter *ca.* 10 mm), and observed whilst slowly heating (or cooling) the tube in a water bath within the range 0–85 °C. The heating/cooling rate was 0.5 °C min⁻¹. The change from a mobile to an immobile system (or *vice versa*) was determined by inverting the tube.

2.3 Small-angle X-ray scattering

SAXS experiments were conducted at the Synchrotron Radiation Source, Daresbury Laboratory, UK, on beamline 2.1.²⁷ Sols and gels were subjected to either steady shear or oscillatory shear using a Couette cell described previously.²⁸ Other details have been reported elsewhere.¹⁹ The X-ray beam was in the radial direction, *i.e.*, it passed through the centre of the Couette cell. Thus SAXS patterns were collected in the (v, e) plane, where v denotes the flow direction and e the neutral (vorticity) direction. A water bath²⁸ enabled investigation of samples under a controlled heating ramp.

Table 1 Molecular characteristics of the block copolymers and the low-concentration limits of their immobile aqueous gels^a

Copolymer	wt.% E (NMR)	$M_n/10^3$ g mol ⁻¹ (NMR)	M_w/M_n (GPC)	c^* (wt.%)	$T^*/^\circ\text{C}$
$E_{96}B_{18}$	77	5.5	1.03	7.5	2
$E_{184}B_{18}$	86	9.4	1.03	4.5	8
$E_{315}B_{17}$	92	15.1	1.04	4.0	15
$E_{398}B_{19}$	93	18.9	1.06	3.5	20

^a Estimated uncertainties: $\pm 3\%$ in M_n and block lengths: ± 0.01 in M_w/M_n . Limiting conditions: c^* to ± 0.2 wt.%, T^* to ± 5 °C.

3 Results

The plots in Fig. 1 show the immobile (hard gel) and mobile regions defined by previous¹⁸ and present (Section 3.1) work. The data points for copolymer E₃₁₅B₁₇ are omitted: gels of this copolymer were studied by rheometry only in the dilute range below the hard-gel region. Features which are useful in considering the results which follow are the temperature range of an immobile gel at any given concentration, and the critical concentration for forming the immobile gel (c^*). This last quantity, together with the related temperature (T^*), is listed in Table 1.

3.1 Storage and loss moduli

3.1.1 Hard gels. The effect of concentration and temperature on the storage modulus at 1 Hz of 5–14 wt.% aqueous gels of copolymer E₁₈₄B₁₈ is shown in Fig. 2. This shows that G' increases monotonically with concentration for all temperatures in the hard-gel range, and that the temperature at which G' falls to a low value is an increasing function of concentration. Comparison of values of $\log(G')$ and $\log(G'')$ showed that the transition to low values of the storage modulus ($G' < 0.5$ kPa) was usually to a soft gel ($G' > G''$), as illustrated in Fig. 3a for the 6 wt.% gel. The exception in this series was the 5 wt.% gel at low temperatures, which became a sol at $T \approx 15^\circ\text{C}$ before forming a soft gel at $T \approx 50^\circ\text{C}$: see Fig. 3b. In Fig. 1, the temperatures at which the storage modulus fell steeply to a value below 1 kPa are compared with those at which the gel became mobile in the tube inversion experiment. Within experimental scatter, the hard-gel boundaries defined by rheometry and the immobile-gel boundaries defined by tube inversion were the same. Similar,

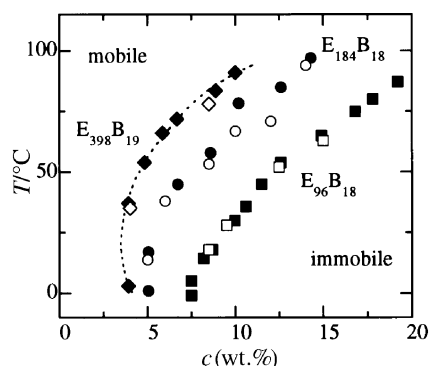


Fig. 1 Phase boundaries for aqueous solutions of block copolymers (squares) E₉₆B₁₈, (circles) E₁₈₄B₁₈ and (diamonds) E₃₉₈B₁₉ determined either by tube inversion (filled symbols) or rheometry (unfilled symbols). The dotted curve shown for sample E₃₉₈B₁₉ was used to define the values of c^* and T^* in Table 1.

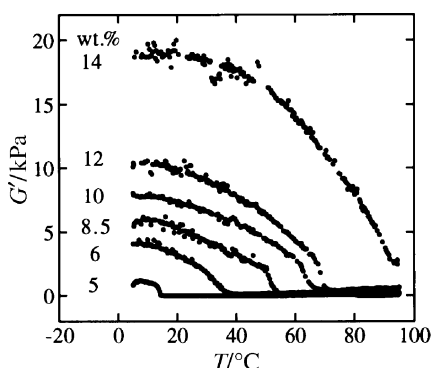


Fig. 2 Temperature dependence of storage modulus ($f = 1$ Hz) for aqueous solutions of block copolymer E₁₈₄B₁₈. Copolymer concentrations (wt.%) are indicated.

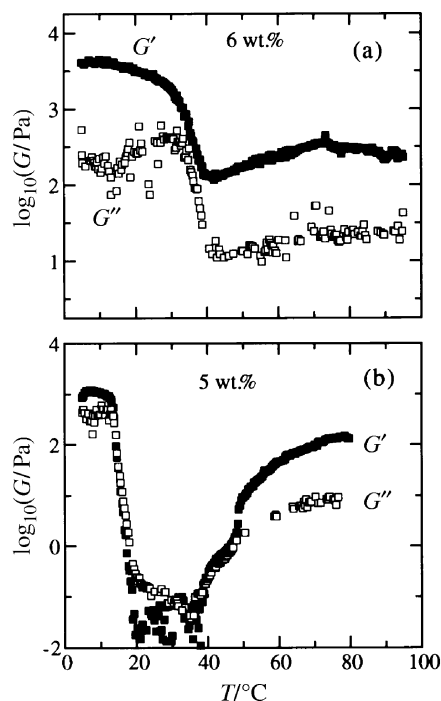


Fig. 3 Temperature dependence of logarithmic storage and loss moduli ($f = 1$ Hz) for aqueous solutions of block copolymer E₁₈₄B₁₈. Filled symbols denote $\log(G')$ and unfilled symbols denote $\log(G'')$. Copolymer concentrations (wt.%) are indicated.

though less extensive, results were obtained for gels of copolymers E₉₆B₁₈ and E₃₉₈B₁₉: see Fig. 1. Considering the combined results, the error in determining temperatures at the hard-gel boundary was estimated to be $\pm 3^\circ\text{C}$.

In Fig. 4, $G'(1 \text{ Hz})$ is plotted against T for the gels of three copolymers at a common concentration, 8.5 wt.%, at which all were hard gels at low temperature and soft gels at high temperature. However, considered in this way the $G'(T)$ curves differ in detail. For those gels with concentration well above the limiting concentration for immobile gel (copolymers E₁₈₄B₁₈ and E₃₉₈B₁₉, $c^* = 4.5$ and 3.5 wt.% respectively, see Fig. 1 and Table 1), the maximum value of G' (at low temperature) decreased as the E-block length was increased. However, the storage modulus of the gel of copolymer E₉₆B₁₈, which at $c = 8.5$ wt.% was near to its $c^* = 7.5$ wt.%, did not fit to this pattern: an explanation is given below. The temperature ranges of the hard gels did follow the trend determined by the tube-inversion experiments (see Fig. 1), *i.e.* the hard-gel phase extended to higher temperatures as the E-block length was increased.

The most dilute immobile gel studied was a 4 wt.% gel of copolymer E₃₉₈B₁₉. The $G'(T)$ curve ($f = 1$ Hz) for that gel is

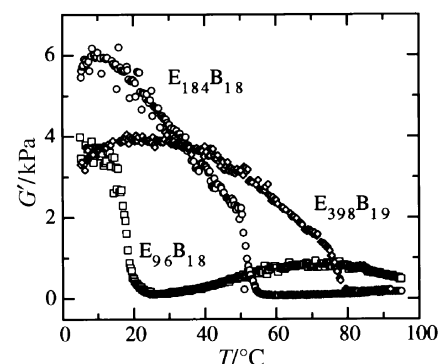


Fig. 4 Temperature dependence of storage modulus ($f = 1$ Hz) for 8.5 wt.% aqueous solutions of block copolymers E₉₆B₁₈, E₁₈₄B₁₈ and E₃₉₈B₁₉ (as indicated).

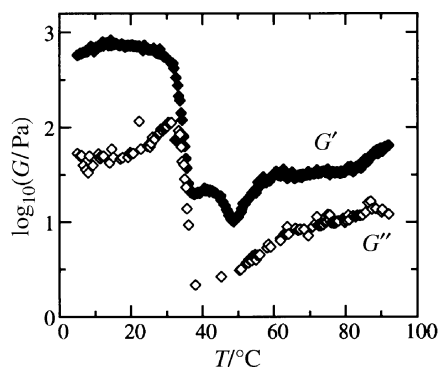


Fig. 5 Temperature dependence of logarithmic storage and loss moduli ($f = 1$ Hz) for a 4 wt.% aqueous solution of block copolymer $E_{398}B_{19}$. Filled symbols denote $\log(G')$ and unfilled symbols denote $\log(G'')$.

shown in Fig. 5, where it is seen that the maximum modulus recorded was only *ca.* 800 Pa. However, the gel in the range $T = 5\text{--}35^\circ\text{C}$ was robust under stress, *i.e.* it could not be disrupted by vigorously shaking its container, consistent with a high yield stress (see Section 3.2). The hard-gel boundary [assessed as the temperature at which $\log(G'')$ fell steeply] was 35°C , in agreement with the tube-inversion results: see Fig. 1.

The moduli of all the hard gels with concentrations well removed from their limiting values were essentially independent of frequency in the range investigated. This is illustrated in Fig. 6 for the 8.5 wt.% gel of $E_{184}B_{18}$ at 5°C : the values of G' increased only slightly with increase in frequency. It is clear that G' of this gel measured at $f = 1$ Hz approached its plateau value (G'_∞) while the corresponding value of G'' approached zero. The moduli of hard gels with concentrations nearer the critical value were more dependent on frequency, as illustrated in Fig. 6 by data for the 8.5 wt.% gel of $E_{96}B_{28}$ at 5°C . This gel was not in the G' -plateau region at $f = 1$ Hz, which explains why its storage modulus at low-temperature is lower than expected (see Fig. 4). Values of G' for gels of similar $c - c^*$ (see Table 1 for values of c^*) rank in regular order. For example, at $c - c^* \approx 1$ wt.%, the values of G' obtained for $E_{96}B_{18}$, $E_{184}B_{18}$ and $E_{398}B_{19}$ were *ca.* 10, 3 and 1 kPa respectively.

3.1.2 Soft gels. Plots of storage modulus (frequency = 1 Hz) against temperature obtained for solutions of copolymer $E_{96}B_{18}$ below the limiting concentration for hard-gel formation ($c^* = 7.5$ wt.%) are shown in Fig. 7a. The increase in modulus at high temperatures indicates formation of a soft gel. This is illustrated for the 7 wt.% gel in Fig. 7b, where it is seen that $G' > G''$ in the high- T region. Maximum values of G' for the high-temperature soft gels of $E_{96}B_{18}$ ranged from 50 to

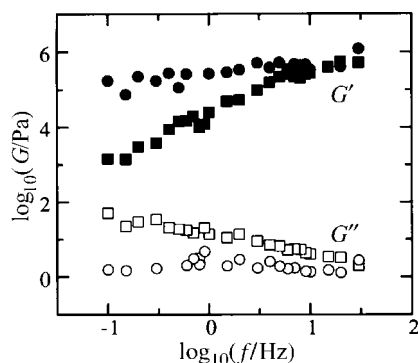


Fig. 6 Frequency dependence of storage and loss moduli for 8.5 wt.% aqueous solutions at $T = 5^\circ\text{C}$ of block copolymers $E_{96}B_{18}$ (squares) and $E_{184}B_{18}$ (circles). Filled symbols denote G' and unfilled symbols denote G'' .

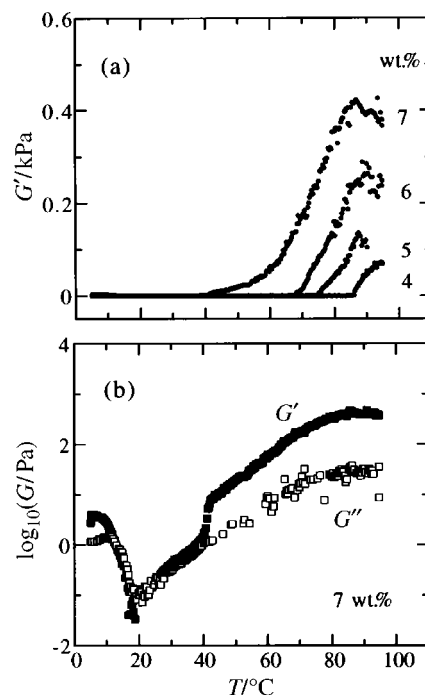


Fig. 7 (a) Temperature dependence of storage modulus ($f = 1$ Hz) for aqueous solutions of block copolymer $E_{96}B_{18}$. Copolymer concentrations (wt.%) are indicated. (b) Temperature dependence of logarithmic storage and loss moduli ($f = 1$ Hz) for a 7 wt.% aqueous solution of block copolymer $E_{96}B_{18}$. Filled symbols denote $\log(G')$ and unfilled symbols denote $\log(G'')$.

450 Pa compared with maximum values well in excess of 1 kPa for the hard gels (see Fig. 4). The maximum at high T in the curves in Fig. 7a point to an upper limit to the soft-gel region, but outside the range of our experiments. The results obtained for the other copolymers in solution at high temperature were similar to those illustrated in Fig. 7.

A low-temperature soft gel was found for the 7 wt.% solution of copolymer $E_{96}B_{18}$ (see Fig. 7b). The maximum value of G' (1 Hz) ≈ 4 Pa measured for this gel was very much lower than that of the corresponding high-temperature soft gel, *i.e.* $G' \approx 450$ Pa at $T \approx 85^\circ\text{C}$. This type of low- T soft gel was not found for any other solution investigated in this work. However, the particular result was repeatedly reproduced using fresh solutions of $E_{96}B_{18}$ of similar composition.

The temperatures at which the $G'(T)$ curves leave the baseline (see Fig. 7a) were used to define the lower boundaries of the soft-gel region of the phase diagram. Unlike the hard-gel boundaries, which were independent of frequency except immediately above the limiting concentrations for the hard gel, the soft-gel boundaries depended significantly on frequency. As an example, Fig. 8 shows the soft-gel/sol boundaries defined for solutions of copolymer $E_{184}B_{18}$ using

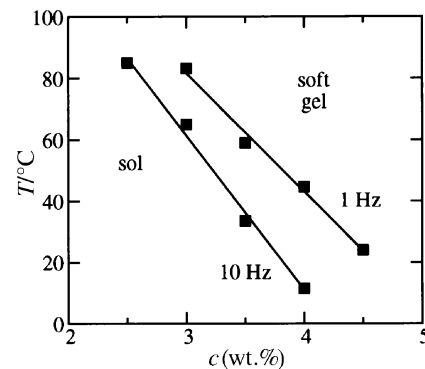


Fig. 8 Frequency dependence of the sol/soft-gel boundary for aqueous solutions of block copolymer $E_{184}B_{18}$.

frequencies of 10 and 1 Hz. As described in Section 3.1.1, the hard-gel boundaries were relatively insensitive to frequency within the range investigated.

The soft-gel/sol boundaries determined from G' measured at 1 Hz are shown in Fig. 9a, together with corresponding hard-gel/soft-gel and hard-gel/sol boundaries. Fig. 9b shows the same data but plotted as $T - T^*$ vs. $c - c^*$, where the limiting conditions for hard-gel formation (c^* and T^*) are taken from Table 1. Data points obtained for copolymer $E_{315}B_{17}$ (not shown in Fig. 9a) are included in this figure. This representation has the advantage of clarity. As noted in Section 3.1.1, the use of $c - c^*$ and $T - T^*$ as determinants of gelation behaviour is useful in interpreting related experimental results.

3.2 Yield stress and viscosity

3.2.1 Hard gels. The effect of temperature on a 6 wt.% aqueous gel of copolymer $E_{184}B_{18}$ subject to a programmed increase in shear stress is shown in Fig. 10. Often the gel fractured under shear, which terminated the program (see Fig. 10). The yield stress (σ_y), defined as that at which the shear rate discernibly left the zero shear rate axis, decreased with increase in temperature. At 35 and 45 °C, above the hard-gel/soft-gel boundary, σ_y fell to low values characteristic of soft gels (see Section 3.2.2). Yield stresses were also measured for the 8.5 wt.% gel of copolymer $E_{96}B_{18}$ and the 4 wt.% gel of copolymer $E_{398}B_{19}$. As for the 6 wt.% gel of copolymer $E_{184}B_{18}$ (Fig. 10), values of σ_y recorded for these hard gels were in the range 40–120 Pa.

The average value of the ratio of $\sigma_y/G'(1 \text{ Hz})$ obtained for gels of $E_{96}B_{18}$ and $E_{184}B_{18}$ (both of which have the fcc structure) is $\sigma_y/G' = 0.029 \pm 0.002$. This value can be com-

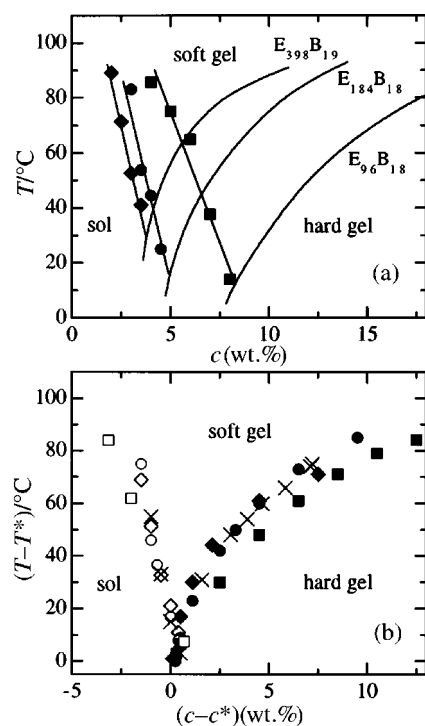


Fig. 9 (a) Phase boundaries for aqueous solutions of block copolymers $E_{96}B_{18}$, $E_{184}B_{18}$ and $E_{398}B_{19}$. The lines denoting the hard-gel boundaries for the three copolymers (as indicated) are taken from Fig. 2. The data points for the soft-gel boundaries are denoted (■) $E_{96}B_{18}$, (●) $E_{184}B_{18}$ and (◆) $E_{398}B_{19}$. (b) Phase boundaries plotted as $T - T^*$ vs. $c - c^*$ for aqueous solutions of block copolymers. Results for (■) $E_{96}B_{18}$, (●) $E_{184}B_{18}$ and (◆) $E_{398}B_{19}$ are taken from (a). Present results for soft gels of copolymer $E_{315}B_{17}$, omitted from (a) for reasons of clarity, are included (denoted ×). The results for hard gels of copolymer $E_{315}B_{17}$ (also denoted ×) are taken from ref. 18.

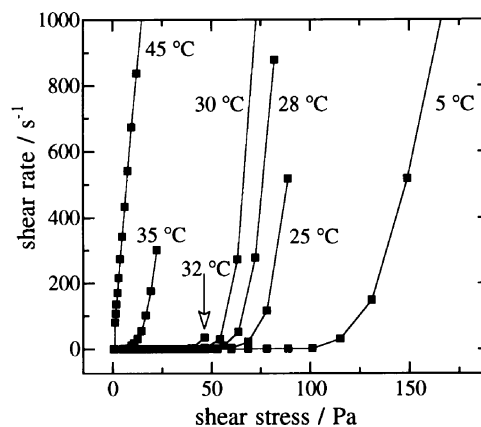


Fig. 10 Effect of shear stress on a 6 wt.% aqueous gel of copolymer $E_{184}B_{18}$ at the temperatures indicated. Termination of the data points indicates fracture of the gel.

pared with those found or predicted for ordered phases of charge-stabilised colloidal dispersions which for a range of systems lie in the range $\sigma_y/G'_\infty = 0.005\text{--}0.03$.²⁹ To the extent that the repulsive 'chain exclusion' potential giving rise to the fcc phase in the present micellar gels can be compared to the double-layer potential in a solution of charged particles, this agreement is most satisfactory.

3.2.2 Soft gels and sols. Examples of shear-stress/shear-rate profiles obtained for a 5 wt.% solution of copolymer $E_{96}B_{18}$ are shown in Fig. 11a. The soft gel at 85 °C has $\sigma_y = 5 \text{ Pa}$, and the sols (45 °C or lower) have no yield stress. The Newtonian viscosities of the sols decrease with increase in temperature, from 9 mPa s at 5 °C to 2 mPa s at 45 °C, *i.e.* approaching that of pure water.

Yield stresses measured for the soft gels were dependent on the time allowed for equilibration of the gel after shearing to break the structure. For example, a 4 wt.% soft gel of copoly-

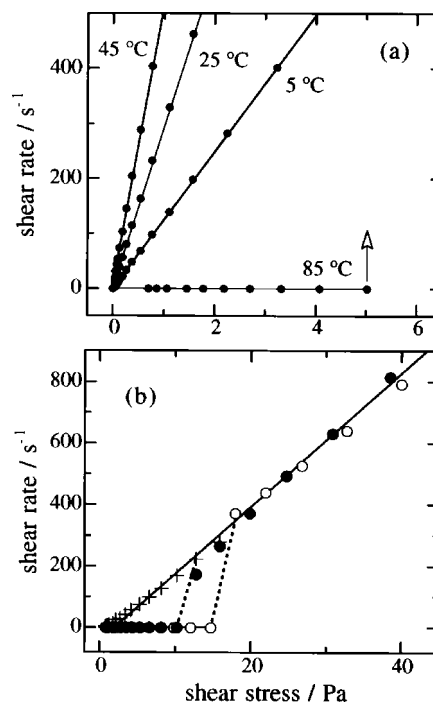


Fig. 11 (a) Effect of temperature on the viscosity of a 5 wt.% aqueous sol of copolymer $E_{96}B_{18}$. At 85 °C the system is a soft gel: the arrow indicates fracture on yield. (b) Effect of equilibration time on the yield stress of a 7 wt.% aqueous soft gel at 5 °C of copolymer $E_{96}B_{18}$. The recovery times after shear were (+) 0, (●) 30 and (○) 60 min. The dashed lines point out the fact that the viscosity immediately after yield is the same irrespective of history.

mer $E_{184}B_{18}$ at 65°C had a yield stress of 8 Pa after equilibrating for 60 min, but a near-zero value if re-measured as quickly as possible after shearing. Hard gels and sols examined in the same way showed no detectable effects of storage time after shearing. The highest yield stress measured across a range of soft gels (including the low- T soft gel of 7 wt.% $E_{98}B_{18}$) was 12 Pa, *i.e.* considerably lower than the values found for the hard gels ($\sigma_y \geq 40$ Pa), and sufficiently so to render the soft gels mobile under the conditions of the tube-inversion test.

After yield of a soft gel at a given temperature, the flow behaviours of the resulting fluids were usually the same irrespective of treatment: see Fig. 11b. However, the profiles of some previously-sheared fluids which had been allowed zero recovery time showed discontinuities attributable to transient structure formation during shear.³⁰

3.3 Gel structures by SAXS

The experiments carried out are summarised in Table 2. For convenience, results reported previously¹⁹ for hard (9–10 wt.%) gels of the four copolymers at 20°C are included.

3.3.1 Hard gels. As discussed previously,¹⁹ 9–10 wt.% hard gels at 20°C (experiments 2, 7, 11 and 15 in Table 2) were characterised as cubic structures formed from packed spherical micelles: fcc for the gels of copolymers $E_{96}B_{18}$ and $E_{184}B_{18}$, and bcc for those of $E_{315}B_{17}$ and $E_{398}B_{19}$. This difference in structure was ascribed to differences in intermicellar interaction in the gel, the micelles with the longer E blocks in their corona acting as softer spheres than those with the shorter E blocks. The structures of the hard gels of the four copolymers at other concentrations (experiments 4, 6, 11, 13, 14) fit into this pattern. A broad correlation for a wide range of E_mB_n diblock copolymers has shown that hard-gel structure is dependent on copolymer concentration, in that dilution at a given temperature favours the transition bcc to fcc.¹⁹ As seen in Table 2 (experiment 10), the 6.5 wt.% hard gel of copolymer $E_{315}B_{17}$ had the fcc structure, whereas (experiment 11) the 10 wt.% hard gel had the bcc structure. The general effect is explained in ref. 19.

3.3.2 Sols. SAXS patterns for sols ($G'' > G'$) of the four copolymers at 20°C are shown in Fig. 12. The concentrations chosen were immediately below the hard-gel limit (c^* in Table 1). Shear had no effect on the two-dimensional diffraction patterns, which remained isotropic throughout the experiments. Therefore, it was convenient to represent the two-dimensional SAXS data reduced to a one-dimensional profile of intensity as a function of q . As can be seen in Fig. 12, apart from copolymer $E_{96}B_{18}$ each sol is characterised by a SAXS pattern containing a single broad peak. The pattern from the

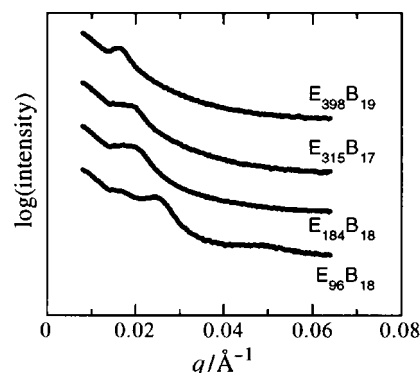


Fig. 12 Intensity profiles obtained by radial integration of isotropic 2-dimensional SAXS patterns from unsheared aqueous sols at 20°C . From top to bottom: 3 wt.% $E_{398}B_{19}$, 4.5 wt.% $E_{315}B_{17}$, 4 wt.% $E_{184}B_{18}$ and 7 wt.% $E_{96}B_{18}$. For clarity, the curves have been shifted on the ordinate scale.

$E_{96}B_{18}$ sol contains a broad secondary maximum at larger q . The single broad peaks indicate that the sols are disordered micellar solutions: the existence of a second-order peak in the pattern from the $E_{96}B_{18}$ sol hints at a more ordered system, possibly linked to the formation of the low-temperature soft gel in that system.

The location of the first maximum (q^*) in the scattering patterns characterises the preferred intermicellar distance (d). The maxima cannot be located precisely, but they correspond to d increasing with E-block length in the approximate range 26–39 nm. These values are significantly larger than those found¹⁹ for the micelles of the same copolymers in well-ordered 9–10 wt.% hard gels at 20°C ($d \approx 23$ –32 nm) and (with the possible exception of the 7 wt.% $E_{98}B_{18}$ sol) are consistent with a single, disordered, sol phase being formed on dilution at 20°C .

3.3.3 Hard-gel/soft-gel transition. SAXS experiments were carried out over a range of temperature for a number of gels, as indicated in Table 2. Transitions from hard to soft gel were most readily located from oriented patterns, *i.e.* as diffuse rings growing at the expense of sharp Bragg peaks. The data obtained for the 6.5 wt.% $E_{184}B_{18}$ gel (Fig. 13a and b) illustrate this gradual decrease in intensity of Bragg reflections, especially of the off-meridional reflections, accompanied by enhancement of diffuse scattering in the ring under the Bragg reflections. In some experiments, in which the sample had been subjected to oscillatory shear, the transition was more evident, as shown by the data for the 4 wt.% $E_{398}B_{19}$ gel (Fig. 13c and d). Within the transition range, peak shift with temperature, if any, was too small to be measured. The uncertainty in the estimated transition temperature between the

Table 2 SAXS results for dilute aqueous sols and gels of E_mB_n block copolymers

	Copolymers	c (wt.%)	$T/^\circ\text{C}$	SAXS	Rheology
1	$E_{96}B_{18}$	7	20–80	Two diffuse rings	Sol \rightarrow soft: 36°C
2		9	20	fcc	Hard
3		9	50	Two diffuse rings	Soft
4	$E_{184}B_{18}$	15	20–80	fcc	Hard \rightarrow soft: 70°C
5		4	20	One diffuse ring	Sol
6		6	20–50	fcc \rightarrow diffuse fcc: 36°C	Hard \rightarrow soft: 38°C
7		10	20	fcc	Hard
8	$E_{315}B_{17}$	4.5	10–40	One diffuse ring	Sol
9		5.5	10–70	One diffuse ring	Hard \rightarrow soft: 45°C
10		6.5	20–80	fcc \rightarrow one diffuse ring: 45°C	Hard \rightarrow soft: 55°C
11	$E_{398}B_{19}$	10	20	bcc	Hard
12		3	20	One diffuse ring	Sol
13		4	5–55	bcc \rightarrow one diffuse ring: 50°C	Hard \rightarrow soft: 35°C
14		5	20–80	bcc \rightarrow one diffuse ring: 44°C	Hard \rightarrow soft: 55°C
15		10	20–95	bcc \rightarrow one diffuse ring: 90°C	Hard

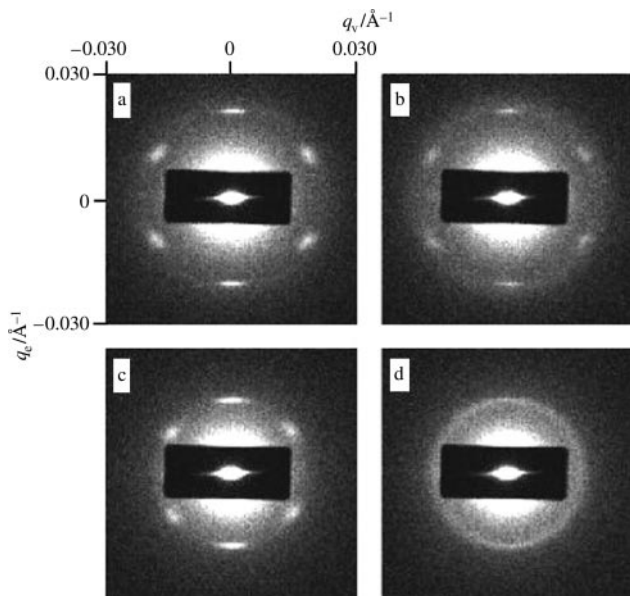


Fig. 13 SAXS patterns for an unsheared 6.5 wt.% gel of copolymer $E_{184}B_{18}$ at (a) 30 °C and (b) 45 °C, and a 4 wt.% gel of copolymer $E_{398}B_{19}$ subjected to oscillatory shear at 50 Hz and 35% amplitude but measured at rest at (c) 40 °C and (d) 55 °C. All patterns are shown with the same gray-scale range.

low- T hard gel and the high- T soft gel was large, at least ± 3 °C. Given a similar uncertainty in temperatures at the hard-gel boundary determined by rheology (± 3 °C, see Section 3.1.1), the results obtained by the two methods are considered to be in fair agreement: see Table 2.

4 Discussion

The formation and structures of the hard gels of the present copolymers have been discussed previously.¹⁹ The present discussion focuses on the soft gels.

4.1 Comparison with $E_{41}B_8$

Considering block copolymers dissolved in water alone, the only other diblock copoly(oxyalkylene) for which soft gels have been identified and studied is $E_{41}B_8$.^{21,25} For convenience in this discussion, the low-concentration region of the $E_{41}B_8$ phase diagram is shown in Fig. 14. The soft-gel regions in the phase diagrams of the present copolymers (see Fig. 9a) are different in extent and position. However, considering the effect of an increase in E-block length on the hard-gel region, the soft-gel regions found for the present copolymers are of necessity moved towards low concentrations. Given the negative slope of the low-temperature sol \rightarrow soft-gel boundary, which is similar for $E_{41}B_8$ and the present copolymers, this

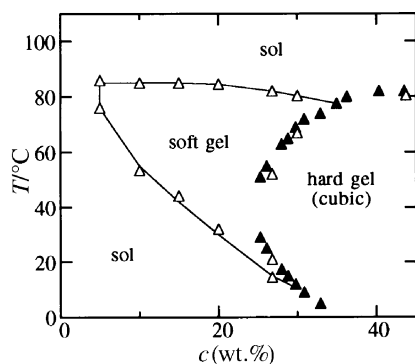


Fig. 14 Phase boundaries for aqueous solutions of copolymer $E_{41}B_8$. The unfilled symbols denote result from rheometry; and the filled circles results from tube inversion.

compression forces that boundary to higher temperatures. In fact the lower limits of the soft-gel region which can be read off Fig. 9a are approximately 12 °C ($E_{96}B_{18}$), 16 °C ($E_{184}B_{18}$) and 30 °C ($E_{398}B_{19}$), compared with 8 °C for $E_{41}B_8$ (Fig. 14).

Indications from rheology are that the upper limit of the soft-gel region is significantly higher than 100 °C (see Fig. 7), whereas it is 85 °C or lower for copolymer $E_{41}B_8$. As for the present copolymers, the high-temperature transition for $E_{41}B_8$ in the low-concentration range ($c < 35$ wt.%) is from hard gel to soft gel (see Fig. 14).

We conclude that the mechanism of soft-gel formation is similar for all five of the diblock copolymers considered, *i.e.* for diblock copolymers with E-block lengths ranging from 41 to 398 E units.

4.2 Triblock copolymers and rod-like micelles

Other copoly(oxyalkylene)s in aqueous solution for which soft gels have been identified have all been triblock copolymers: *i.e.* $E_{27}P_{39}E_{27}$ (P85),¹¹ $E_{21}P_{47}E_{21}$ (P94)¹² and $E_{16}B_{10}E_{16}$.³¹ For P85 there is ample evidence (including results from light scattering, viscometry, SANS and SAXS) for the formation of cylindrical micelles at high temperatures (> 80 °C) in water^{7,8,32–34} and at lower temperatures in salt solution (a poorer solvent).¹² For P94¹¹ the evidence is less direct. For both systems the rheological properties of the soft gel are attributed to the hindered rotation of rod-like micelles.^{11,12} There is also viscometric evidence of a sphere-to-rod transition at $T \approx 60$ °C in dilute aqueous solutions of copolymer $E_{16}B_{10}E_{16}$, and at moderately-concentrated solution (*e.g.*, 30 wt.%) the micellar solutions of this copolymer do form soft gels. However, in this case soft gel forms at temperatures below the sphere-to-rod transition temperature ($T \approx 60$ °C), and transforms to a sol above that temperature. It is relevant that the first-formed (*i.e.* lowest concentration) hard gel of $E_{16}B_{10}E_{16}$ comprises hexagonally-packed cylindrical micelles³¹ which is similar to hard gels formed from other $E_mP_nE_m$ copolymers with short E blocks (*e.g.* $E_{12}E_{27}E_{12}$, $E_{13}P_{30}E_{13}$ and $E_{20}P_{30}E_{20}$)⁶ and from P85 itself at high temperatures,³⁵ although the assignment of hard-gel structures in this case has been questioned.³³

4.3 Soft-gel formation in diblock copolymers

Returning to discussion of diblock copoly(oxyalkylene)s with E-block lengths of 40 units or more, we know of no evidence supporting a sphere-to-rod transition in their micellar solutions in water alone. The concentration-induced hard-gel transition from cubic-packed spherical micelles to hexagonally-packed cylindrical micelles found for copolymer $E_{41}B_8$ at high concentration ($c > 50$ wt.%)^{21,25} is the well-known effect of packing density.³⁶ A temperature-induced sphere-to-rod transition has been detected (by SAXS) at $T \approx 70$ °C for gels of copolymer $E_{41}B_{10}$ in salt solution, the high-temperature gel in that case being characterised as hexagonally-packed cylindrical micelles.^{37,38} However, in the same system the mobile phase accessed at temperatures immediately above the upper hard-gel boundary was characterised as a defect cubic phase (spherical micelles, defect fcc). Hard gels of copolymer $E_{90}B_{10}$ in water (30 to 60 wt.%) have been shown by SAXS to be cubic-packed spheres from 25–70 °C,¹⁶ while similar experiments for a 25 wt.% gel of copolymer $E_{86}B_{10}$ in salt solution accessed a high-temperature cloudy-gel phase which gave SAXS patterns from a bcc structure up to 90 °C.^{16,39,40}

A 30 wt.% hard gel of copolymer $E_{106}B_{16}$ examined by SAXS from 25–75 °C also provided consistent evidence of the bcc structure.⁴¹ Finally, considering dilute solutions (1–2 wt.%), SANS has been used to show that micelles of copolymer $E_{86}B_{10}$ in water are spherical at temperatures up to 70 °C.¹⁶

4.3.1 Hard-gel/soft-gel transition. Given the evidence outlined above, for the present copolymers it is reasonable to assign the soft gels formed at temperature above the upper hard-gel boundary to defect cubic (bcc or fcc) structures of spherical micelles. As discussed previously,³⁹ defects allow grains of ordered phase to slip past each other, and the system can become mobile whilst still giving a diffuse SAXS pattern consistent with the sharper pattern obtained from the hard-gel structure. The SAXS evidence summarised in Table 2 lends support to this assignment. In several experiments (denoted 4, 6 and 13 in Table 2), cubic structure was identified in the soft gel formed immediately above the hard-gel \rightarrow soft-gel transition temperature. A similar result was obtained on heating a 40 wt.% hard gel of copolymer E₄₁B₈ through its upper hard-gel boundary.²⁵ In other experiments with the present copolymers (10, 14 and 15 in Table 2) there was evidence of degradation of the cubic structure on heating within the hard-gel region, and in one experiment (9 in Table 2) evidence of a well-ordered cubic structure for the hard gel was entirely lacking.

4.3.2 Sol/soft-gel transition. The SAXS experiments carried out in the present work included only one (experiment 1) covering the sol \rightarrow soft-gel transition. No evidence of a change in structure was noted. However, as discussed above, the formation of soft gel at low concentrations of the diblock copolymers demands a broader interpretation than that applied to the P85 and P94 systems by Hvidt and co-workers,^{11,12} i.e. soft gel formed from rod-like micelles. There is no evidence to support the formation of rod-like micelles in the present and closely-related systems. The alternative is a soft gel formed from spherical micelles. As suggested previously for soft gels in solutions of copolymer E₄₁B₈,²¹ the soft gel could contain structures of weakly-interacting spherical micelles in dynamic equilibrium, such that the transition from sol to soft gel occurs when micellar aggregates with fractal geometry reach a percolation threshold yielding sufficient structure to cause, at a given frequency, the dynamic storage modulus to exceed the loss modulus. For this mechanism to hold, micellar aggregation must be enhanced at high temperature. This is indeed the case, since on heating water becomes a poorer solvent for the E-block of the corona.

Recently, results obtained by small-angle neutron scattering (SANS) have been used to define a percolation boundary in the phase diagram for 10–25 wt.% aqueous solutions of triblock copolymer E₁₃P₃₀E₁₃ (coded L64).⁴² The boundary was obtained by interpreting the SANS data using a modification of Baxter's sticky-sphere model,^{43,44} and finding points on the phase diagram at which the stickiness parameter increased abruptly. The resulting percolation boundary (see Fig. 1 of ref. 44) is a similar shape to the sol/soft-gel boundaries shown in Fig. 9, though at higher concentration. Results from rheometry, used to check the 'SANS' boundary by way of an abrupt rise in modulus, differ from the present results in that G' did not exceed G'' above the L64 percolation threshold. There are other differences to take into account, not least the fact that macrophase separation (clouding) was not encountered in the present system whereas it occurs at approximately 60 °C in micellar solutions of L64. It remains to be seen whether a sticky-sphere model can explain the totality of available data. Nevertheless, we take the qualitative agreement between the systems as support for our interpretation of soft-gel formation on heating aqueous solutions of the present E_nB_n as a percolation transition. Further experiments are planned to provide additional evidence for this, including measurements of the frequency dependence of the dynamic shear moduli. A power law dependence on frequency is expected at the gel point based on the Winter–Chambon method of determining the onset of gelation.⁴⁵ If the critical gel has a percolated fractal structure, the power law exponent

can be related to the fractal dimension, which can be obtained independently from SAXS.

It remains to comment on the formation of a soft gel at low temperature in the 7 wt.% solution of E₉₆B₁₈ (see Section 3.1.2 and Fig. 7b). The effect of lowering temperature is a better solvent for the E-block and a consequent expansion of the micelle corona. This will increase the effective volume fraction of micelles in solution. At an appropriate micelle volume fraction, soft gel ($G' > G''$) is reformed, possibly by packing, possibly by percolation. It follows that an increase in temperature will decrease the effective volume fraction and give a sol. As discussed above, further increase in temperature eventually leads to formation of a second soft gel (see Fig. 7b), presumably by a percolation mechanism. The fact that the low- T soft gel was found for only one of the many solutions investigated points to a very delicate balance between copolymer concentration and temperature for the effect to occur.

4 Conclusions

The following summary applies to the four diblock copolymers E₉₆B₁₈, E₁₈₄B₁₈, E₃₁₅B₁₇ and E₃₉₈B₁₉, i.e. systems with a common B-block length and lengthy E blocks. They will not apply in detail to other diblock copolymers of the E_mB_n system, although the general trends should hold.

Immobile hard gels (high modulus, high yield stress) and mobile soft gels (low modulus, low yield stress, $G' > G''$) form in aqueous solutions of all four copolymers. The increase in E-block length from 96 to 398 repeat units has the overall effect of moving both hard and soft-gel phases to lower concentrations without changing the pattern of behaviour. The exception is the hard-gel structure, which is fcc at short E-block lengths but bcc at long E-block lengths.¹⁹

For hard gels at concentrations well above c^* , the maximum value of G' decreases as the E-block length is increased. The yield stress (σ_y) follows the same trend, the two being closely correlated, with the ratio $G'/\sigma_y \approx 0.03$. Values of G' and σ_y become lower as c^* is approached.

The hard gels transform to soft gels at high temperature. Most probably the soft gel in this region of the phase diagram has a defect bcc or fcc structure. At concentrations below c^* , soft gels form from sols as the temperature is increased. In this region the soft gels most probably form when the system passes through its percolation threshold.

Considering the complete phase diagram, the critical conditions for hard-gel formation (c^* , T^*) serve as parameters for the production of a 'universal' phase diagram covering both hard and soft gels.

Acknowledgements

WM was supported by the Thai Government, and AK and CD by the EU-TRM network 'Complex Architectures in Diblock Based Copolymer Systems'. Support for polymer synthesis and SAXS at the Daresbury facility was through EPSRC grants GR/L22645 and GR/L79854.

References

- 1 B. Chu and Z.-K. Zhou, in *Nonionic Surfactants: Polyoxyalkylene Block Copolymers*, ed. V. M. Nace, Marcel Dekker Inc., New York, 1996, ch. 3.
- 2 M. Almgren, W. Brown and S. Hvidt, *Colloid Polym. Sci.*, 1995, **273**, 2.
- 3 K. Mortensen, *Curr. Opin. Colloid Interface Sci.*, 1998, **3**, 12.
- 4 I. R. Schmolka and L. R. Bacon, *J. Am. Oil Chem. Soc.*, 1967, **44**, 559.
- 5 G. Wanka, H. Hoffmann and W. Ulbricht, *Colloid Polym. Sci.*, 1990, **268**, 569.
- 6 G. Wanka, H. Hoffmann and W. Ulbricht, *Macromolecules*, 1994, **27**, 4145.
- 7 K. Mortensen and W. Brown, *Macromolecules*, 1993, **26**, 4128.
- 8 K. Mortensen and J. S. Pedersen, *Macromolecules*, 1993, **26**, 805.

- 9 K. Mortensen and Y. Talmon, *Macromolecules*, 1995, **28**, 805.
- 10 K. Mortensen, *J. Phys. Condens. Matter*, 1996, **8**, A103.
- 11 S. Hvidt, E. B. Jørgensen, W. Brown and K. Schillen, *J. Phys. Chem.*, 1994, **98**, 12320.
- 12 E. B. Jørgensen, S. Hvidt, W. Brown and K. Schillen, *Macromolecules*, 1997, **30**, 2355.
- 13 J. Noolandi, A.-C. Shi and P. Linse, *Macromolecules*, 1995, **29**, 5907.
- 14 Y.-W. Yang, Z. Ali-Adib, N. B. McKeown, A. J. Ryan, D. Attwood and C. Booth, *Langmuir*, 1997, **13**, 1860.
- 15 The Dow Chemical Co., Freeport, Texas, *Technical Literature, B-Series Polyglycols. Butylene Oxide/Ethylene Oxide Block Copolymers*.
- 16 L. Derici, S. Ledger, S.-M. Mai, C. Booth, I. W. Hamley and J. S. Pedersen, *Phys. Chem. Chem. Phys.*, 1999, **1**, 2773.
- 17 P. Alexandridis, U. Olsson and B. Lindman, *Langmuir*, 1997, **13**, 23.
- 18 W. Mingvanish, S.-M. Mai, F. Heatley, C. Booth and D. Attwood, *J. Phys. Chem.*, 1999, **103**, 11269.
- 19 I. W. Hamley, C. Daniel, W. Mingvanish, S.-M. Mai, C. Booth, L. Messe and A. J. Ryan, *Langmuir*, 2000, **16**, 2508.
- 20 B. Nyström and H. Walderhaug, *J. Phys. Chem.*, 1996, **100**, 5433.
- 21 H. Li, G.-E. Yu, C. Price, C. Booth, E. Hecht and H. Hoffmann, *Macromolecules*, 1997, **30**, 1347.
- 22 A. D. Bedells, R. M. Arafah, Z. Yang, D. Attwood, J. C. Padget, C. Price and C. Booth, *J. Chem. Soc., Faraday Trans.*, 1993, **89**, 1243.
- 23 S. Tanodekaew, N.-J. Deng, S. Smith, Y.-W. Yang, D. Attwood and C. Booth, *J. Phys. Chem.*, 1993, **97**, 11847.
- 24 N.-J. Deng, Y.-Z. Luo, S. Tanodekaew, N. Bingham, D. Attwood and C. Booth, *J. Polym. Sci., Part B: Polym. Phys.*, 1985, **33**, 1085.
- 25 J. P. A. Fairclough, A. J. Ryan, I. W. Hamley, H. Li, G.-E. Yu and C. Booth, *Macromolecules*, 1999, **32**, 2058.
- 26 W. Mingvanish, A. Kelarakis, S.-M. Mai, C. Daniel, Z. Yang, V. Havredaki, I. W. Hamley, A. J. Ryan and C. Booth, *J. Phys. Chem. B*, submitted.
- 27 E. Towns-Andrews, A. Berry, J. Bordas, G. R. Mant, P. K. Murray, K. Roberts, I. Sumner, J. S. Worgan, E. Lewis and A. Gabriel, *Rev. Sci. Instrum.*, 1989, **60**, 2346.
- 28 J. A. Pople, I. W. Hamley and G. P. Diakun, *Rev. Sci. Instrum.*, 1998, **69**, 3015.
- 29 See R. G. Larson, *The Structure and Rheology of Complex Fluids*, Oxford University Press, Oxford, 1999, p. 303, and references therein.
- 30 P. D. Olmsted, *Europhys. Lett.*, 1999, **48**, 339.
- 31 G.-E. Yu, H. Li, J. P. A. Fairclough, A. J. Ryan, N. B. McKeown, Z. Ali-Adib, C. Price and C. Booth, *Langmuir*, 1998, **14**, 5782.
- 32 K. Schillen, W. Brown and R. M. Johnsen, *Macromolecules*, 1994, **27**, 4825.
- 33 O. Glatter, G. Scherf, K. Schillén and W. Brown, *Macromolecules*, 1994, **27**, 6046.
- 34 S. M. King, R. K. Heenan, V. M. Cloke and C. Washington, *Macromolecules*, 1997, **30**, 6215.
- 35 K. Mortensen, *Europhys. Lett.*, 1992, **19**, 599.
- 36 See, for example, D. J. Mitchell, G. J. T. Tiddy, L. Waring, T. Bostock and M. P. M. McDonald, *J. Chem. Soc., Faraday Trans. 1*, 1993, **79**, 975.
- 37 J. A. Pople, I. W. Hamley, J. P. A. Fairclough, A. J. Ryan, B. U. Komanschek, A. J. Gleeson, G.-E. Yu and C. Booth, *Macromolecules*, 1997, **30**, 5721.
- 38 J. A. Pople, I. W. Hamley, N. J. Terrill, J. P. A. Fairclough, A. J. Ryan, G.-E. Yu and C. Booth, *Polymer*, 1998, **39**, 4891.
- 39 I. W. Hamley, J. A. Pople, J. P. A. Fairclough, A. J. Ryan, C. Booth and Y.-W. Yang, *Macromolecules*, 1998, **31**, 3906.
- 40 I. W. Hamley, J. A. Pople, C. Booth, L. Derici, M. Impéror-Clerc and P. Davidson, *Phys. Rev. E*, 1998, **58**, 7620.
- 41 A. Kelarakis, V. Havredaki, L. Derici, G.-E. Yu, C. Booth and I. W. Hamley, *J. Chem. Soc., Faraday Trans.*, 1998, **94**, 3639.
- 42 L. Lobry, N. Micali, F. Mallamace, C. Liao and S.-H. Chen, *Phys. Rev. E*, 1999, **60**, 7076.
- 43 R. J. Baxter, *J. Chem. Phys.*, 1968, **49**, 2770.
- 44 Y. C. Liu, S.-H. Chen and J. S. Huang, *Macromolecules*, 1998, **31**, 2236.
- 45 H. H. Winter and M. Mours, *Adv. Polym. Sci.*, 1997, **134**, 165.